geoconvention
Calgary • Canada • June 20-22 2022

Passive source location by diffraction scanning

Jorge E. Monsegny[1], Don C. Lawton[1,2] and Daniel Trad[1]

[1]CREWES, University of Calgary; [2]Carbon Management Canada

Summary

During CO_2 injection monitoring several events generated by passive sources at different locations are recorded. Some events are from surface operations while others are a consequence of CO_2 injection. We use a technique that analyzes the moveout of the passive seismic events for a series of potential sources located at different positions in the subsurface. The technique generates a plot that catalogs the events by source location making it possible to discern events produced the zone of interest from events generated elsewhere. We apply the technique to passive seismic records at the Containment and Monitoring Field Research Station in Alberta, Canada.

Introduction

CO_2 injection can cause fracturing (Yew and Weng, 2015) and this fracturing can manifest itself in passive seismic records. For this reason, it is important to monitor the seismic activity in a CO_2 injection facility and look for microseismic events generated in the injection zone.

CaMI-FRS stands for Containment and Monitoring Institute Field Research Station. It is a research facility located near Brooks in Alberta, Canada where small volumes of CO_2 are being injected yearly at a depth close to 300m (Macquet et al., 2019). To monitor the reservoir state during the injection a set of technologies are deployed there like multicomponent geophone arrays, distributed acoustic sensing (DAS) and electrical resistivity arrays, both at the surface and inside two observation wells located close to the injection well (Lawton et al., 2017).

In this report we use a technique that analyzes the moveout from several potential seismic sources and catalogs the events in a passive seismic record by the probable source depth. In this way we can distinguish seismic events generated at the surface from the ones generated in the CO_2 injection zone.

First, we are going to show the moveout analysis technique concept with a synthetic experiment. Then we are going to use the technique in a series of passive records from CaMI-FRS where the events from surface operations can be separated from potential events from the CO_2 injection zone.

Methods

Figure 1 shows the velocity model at CaMI-FRS obtained from well data. The circles below the lateral position 250m and from 191m to 306m deep each 5m are the locations of the receiver array inside the observation well. The asterisks below the 300m lateral position are the locations of six passive sources that are going to be used to illustrate the moveout analysis. Their vertical coordinates go from 50m deep to 300m deep every 50m. The same figure, on the right, shows the moveout curves from the sources to the receiver array.

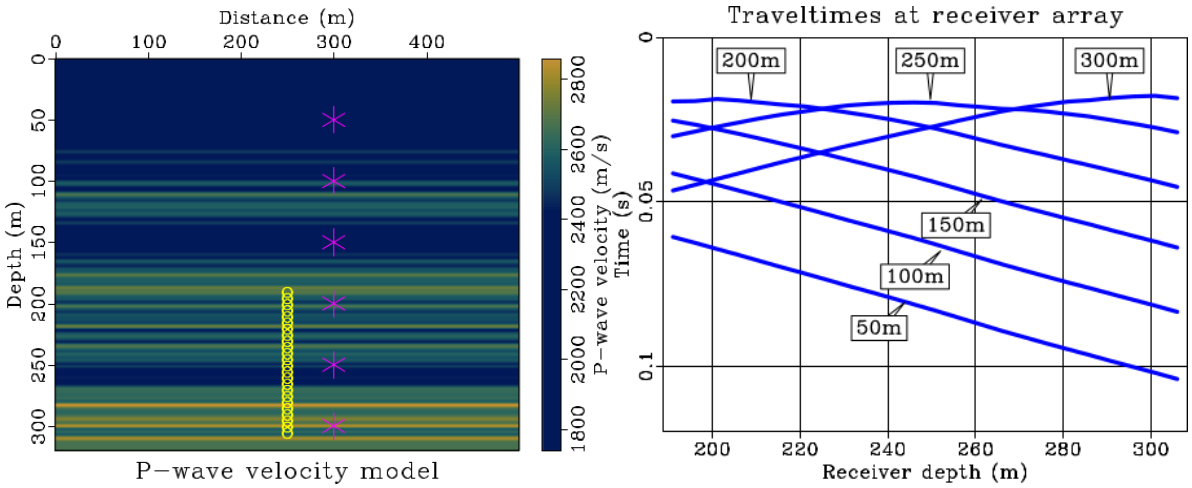

Figure 1. On the left, the velocity model at CaMI-FRS obtained from well data. Superimposed are the geophone locations inside the well (circles) and six passive sources (asterisks) used to illustrate the moveout analysis. On the right, the traveltimes of moveout curves from the sources to the receiver array.

In the left part of Figure 2 is the synthetic shot gather. Each event corresponds to one of the six sources in Figure 1. Each source was activated in sequence from top to bottom, with a small time between them to avoid the events crossing each other.

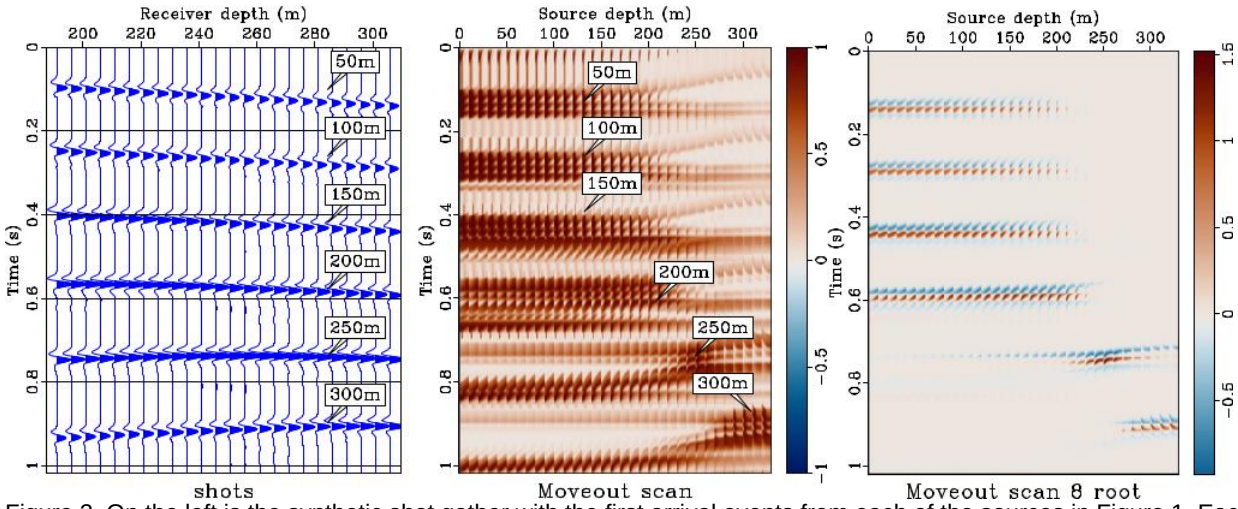

Figure 2. On the left is the synthetic shot gather with the first arrival events from each of the sources in Figure 1. Each event is labelled with the source depth. On the right is the moveout scan plot of the synthetic shot gather with labels showing the semblance highest value zone of each event. On the right is the 8-th root stack.

Each traveltime curve is used as a static correction and is applied to the shot gather. After applying the static corrections, the events that correspond to the moveout curve align horizontally while the others have some angle with respect to the horizontal. This horizontal alignment increases the lateral similarity of the traces. We use the semblance to measure this similarity. The semblance S_T at time t is defined as:

$$S_T(t) \stackrel{\text{def}}{=} \frac{\sum_{\tau=t-m\Delta}^{t+m\Delta} \left(\sum_{i=1}^{N} g_{\tau,i}\right)^2}{N \sum_{\tau=t-m\Delta}^{t+m\Delta} \sum_{i=1}^{N} (g_{\tau,i})^2}, \quad (1)$$

where $m\Delta$ defines a small time window around t, N is the number of traces and $g_{\tau,i}$ is the sample at trace i and time τ (Sheriff, 2002). Semblance values are between 0 and 1 and it can be proved that they are 1 when the traces are equal (Geldart and Sheriff, 2004).

It is usual that the source position is unknown. For that motive we generate moveout curves for a set of sources in an area around the receiver array. In this synthetic example we use sources from 0m to 250m every 10m in the lateral direction and from 0m to 320m every 10m in the vertical direction.

The central part of Figure 2 shows the moveout scan plot of the synthetic gather. This plot is composed of a series of depth stripes and inside each stripe there are semblances for different horizontal positions. The events from sources at 50m to 200m deep have high semblance values for sources between 0m and 200m. In contrast, the events from sources at 250m and 300m deep have more localized semblance values around their true source depths.

Kanasewich et al. (1973) proposed the n-th root stack method to enhance the events while reducing random noise. This method stacks the signed n-th root data amplitude first:

$$r'_n(t) = \frac{1}{N} \sum_{i=1}^{N} |g_{t,i}|^{1/n} sign(g_{t,i}) \quad (2)$$

and then restores the signed amplitudes after stacking:

$$r_n(t) = |r'_n(t)|^n sign(r'_n(t)) \quad (3)$$

with the same notation as before. Figure 2, on the right, displays the results of this technique with n=8. This technique shows better the position of the sources but at the expense of the low energy events.

Field Data

We used data from CaMI-FRS to test the moveout scan technique. The velocity model and receiver array are the same of Figure 1. We also scanned the same set of sources than in the synthetic example and that means that we used again the precomputed moveout curves.

The CaMI-FRS observation well receiver array is composed of multicomponent geophones and we analyze the vertical component because it is the most energetic. Due that the potential sources have different depths with respect to the array, a polarity change is expected in this component. This polarity change is akin to the one observed in active surface seismics in the inline component.

To address this complication, during each semblance calculation we reversed the polarity of the seismic gather below the source depth. This works when the velocity model is simple but when not, an approach that detects the moveout local maxima and minima and reverse the traces between them can be implemented.

The left part of figures 3 and 4 show a portion of a passive seismic record. The only preprocessing was the deletion of some very noisy traces and the application of a 5−50Hz filtering to suppress high frequency noise.

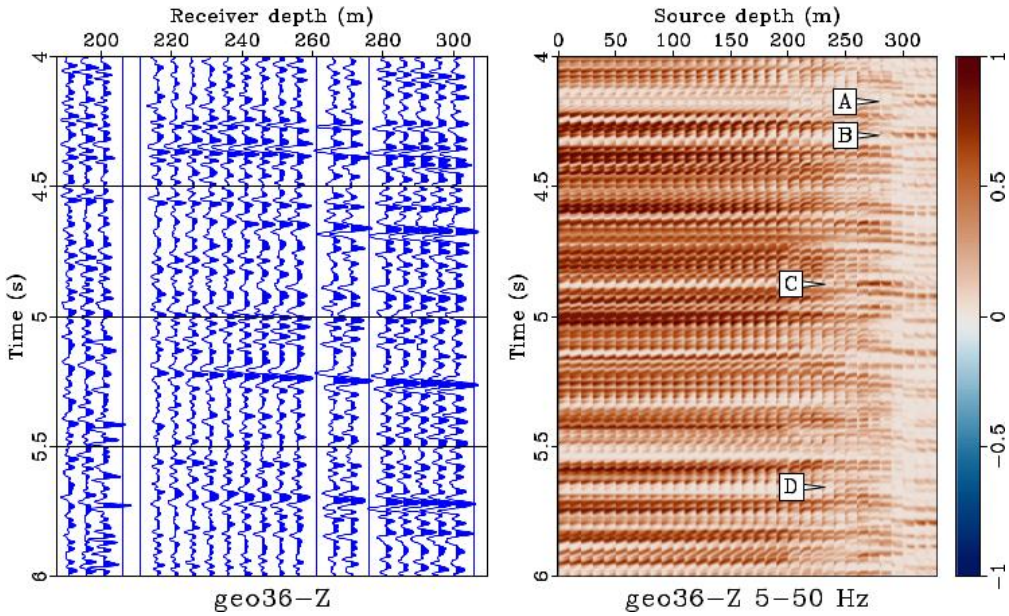

Figure 3. Passive seismic record and moveout semblance plot. The most important features in the record have high semblance values above 200m. Other features, labelled A through D have high semblance values below 200m.

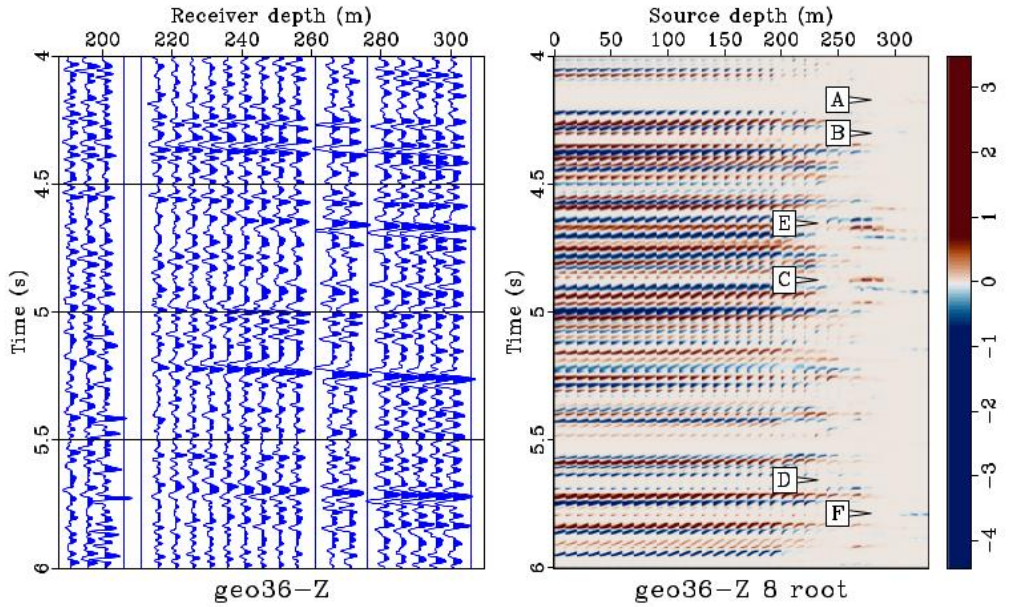

Figure 4. Passive seismic record and moveout 8-th root stacking plot. The most important features in the record have high semblance values above 200m. Other features, labelled A through D have high semblance values below 200m. Feature labelled F is another possible event.

Several events are evident in the seismic record and by following them horizontally to the moveout plot on the right part of the same figures it can be seen that their probable sources are located in a broad area above 200m.

In contrast, some parts of the moveout plot shows probable events below 200m. Events labelled A and B have potential sources below 300m while the ones labelled C and D have sources between 250m and 300m. Although their semblance values are high the actual seismic events in the gather are faint.

Discussion

The moveout plots can distinguish events generated below and above 200m deep. This is due to the aperture of the receiver array. In the future we plan to use DAS data that spans all the well to increase the moveout resolving power.

Several artifacts appear in the moveout plots in Figure 2. They are due to the sidelobes and the semblance normalization effect. A careful interpretation of this plot is needed.

The Radon Transform (Durrani and Bisset, 1984) can detect linear and parabolic events in seismic records. However, it does not manage general velocity models like the moveout plot and does not convey the source locations.

For events generated above 200m the semblance plot gives a very wide source location. This can also be fixed by increasing the receiver array aperture.

Acknowledgements

We thank the sponsors of CREWES for continued support. This work was funded by CREWES industrial sponsors and NSERC (Natural Science and Engineering Research Council of Canada) through the grant CRDPJ 543578-19. The data were acquired through a collaboration with Containment and Monitoring Institute (CaMI) of Carbon Management Canada (CMC). Research at the CaMI field site is supported in part by the Canada First Research Excellence Fund, through the Global Research Initiative at the University of Calgary and the CaMI.FRS Joint Industry Project. The first author (JM) is also supported by Canada First Research Excellence Fund, through the Global Research Initiative at the University of Calgary

References

Durrani, T. S., and D. Bisset, 1984, The radon transform and its properties: GEOPHYSICS, 49, 1180–1187.

Geldart, L. P., and R. E. Sheriff, 2004, Problems in exploration seismology and their solutions: Society of Exploration Geophysicists.

Kanasewich, E. R., C. D. Hemmings, and T. Alpaslan, 1973, Nth-root stack nonlinear multichannel filter: GEOPHYSICS, 38, 327–338

Lawton, D., M. Bertram, A. Saeedfar, M. Macquet, K. Hall, K. Bertram, K. Innanen, and H. Isaac, 2017, DAS and seismic installations at the CaMI Field Research Station, Newell County, Alberta: Technical report, CREWES.

Macquet, M., D. C. Lawton, A. Saeedfar, and K. G. Osadetz, 2019, A feasibility study for detection thresholds of CO2 at shallow depths at the CaMI Field Research Station, Newell County, Alberta, Canada: Petroleum Geoscience, 25, 509–518.

Sheriff, R. E., 2002, Encyclopedic dictionary of applied geophysics, fourth edition: Society of Exploration Geophysicists.

Yew, C. H., and X. Weng, 2015, Mechanics of hydraulic fracturing (second edition), second edition ed.